



A hybrid polyketone–SiO₂ support for palladium catalysts and their applications in cinnamaldehyde hydrogenation and in 1-phenylethanol oxidation



Claudia Antonetti ^a, Luigi Toniolo ^b, Gianni Cavinato ^c, Claudia Forte ^d, Chiara Ghignoli ^a, Randa Ishak ^e, Fabrizio Cavani ^f, Anna Maria Raspolli Galletti ^{a,*}

^a Department of Chemistry and Industrial Chemistry, University of Pisa, Via G. Moruzzi 3, 56124 Pisa, Italy

^b Department of Molecular Sciences and Nanosystems, University Ca' Foscari of Venice, Dorsoduro 2137, 30123 Venice, Italy

^c Department of Chemical Sciences, University of Padua, Via Marzolo 1, 35131 Padua, Italy

^d ICCOM CNR, via G. Moruzzi 1, 56124 Pisa, Italy

^e Department of Civil and Industrial Engineering, Largo Lucio Lazzarino 2, 56126 Pisa, Italy

^f Department of Industrial Chemistry "Toso Montanari", University of Bologna, Viale Risorgimento 4, 41036 Bologna, Italy

ARTICLE INFO

Article history:

Received 30 July 2014

Received in revised form 22 January 2015

Accepted 28 January 2015

Available online 28 February 2015

Keywords:

Hybrid materials

Polyketone–SiO₂

Pd catalysts

Hydrogenation

Oxidation

ABSTRACT

An organic–inorganic hybrid material, PK–SiO₂ (PK = polyketone), was employed as support for Pd catalysts. Their synthesis was carried out by MW irradiation of an ethanol solution of Pd(OAc)₂ in the presence of the support. The obtained systems were characterized by solid state NMR, SEM, TEM, ICP, XPS, BET, gas porosimetry and tested in two probe reactions: the selective hydrogenation of cinnamaldehyde to hydrocinnamaldehyde carried out in decalin and the oxidation of 1-phenylethanol to acetophenone in water. For comparison, Pd/PK and Pd/SiO₂ catalysts were also prepared by using the same procedure, characterized and tested in the same reactions. On the hybrid support the Pd nanoparticles resulted significantly smaller and with a more homogeneous size distribution compared to those on bare SiO₂ or PK. The catalysts on the hybrid support allowed a higher performance and could be recycled up to five times without loss of activity and metal leaching. These results were related to the improved surface area of the hybrid material (compared to the low surface area of bare PK) ascribable to silica introduction, combined with the stabilizing effect of the polymeric counterpart against Pd nanoparticles agglomeration.

© 2015 Published by Elsevier B.V.

1. Introduction

Palladium nanostructured catalysts find many catalytic applications and their performances depend on their size, shape and ability to avoid agglomeration [1,2]. Polymeric stabilizers, such as poly-(1-vinylpirrolidone), polypyrrole, nafion and also natural polymers, are generally employed in order to prevent the agglomeration of Pd colloids towards the bulk metal [3,4]. The obtained “quasi” homogeneous metal nanoparticles offer the same high catalytic activity as the homogeneous ones, however they are not as easily separated and recycled. To overcome these drawbacks, they are generally supported on inorganic carriers.

On the contrary, the application of polymers as supports has been investigated to a lower extent, due to many disadvantages,

such as decrease in thermal, mechanical and chemical stability, shrinking phenomena, changes of volume and porosity that can adversely influence their overall performances [5–8]. Recently, PKs, being high temperature melting materials, insoluble in the most common solvents, have been successfully proposed by us as support for palladium catalysts [9]. PK can act not only as mere support, but also as stabilizing agent through interactions of its keto groups with the Pd nanoparticles without suppressing the catalysis, differently from other polymeric supports. Unfortunately, PKs present a low surface area and scarce compatibility with hydroxylated media, such as water, the eco-friendly medium par excellence. The incorporation of high surface area hydrophilic SiO₂ into PK could overcome these drawbacks and also improve the mechanical properties and stability of the resulting composites [10–13]. So far, a hybrid PK–SiO₂ material has been employed for the preparation of new fuel cell membranes [14], but has never been tested as a catalyst support. These considerations prompted us to prepare some Pd nanostructured catalysts supported on the hybrid PK–SiO₂.

* Corresponding author. Tel.: +39 050 2219290; fax: +39 050 2219260.
E-mail address: anna.maría.raspolli.galletti@unipi.it (A.M. Raspolli Galletti).

material, obtained by carrying out the synthesis of PK in the presence of high surface area Aerosil 380 SiO₂, aiming also at their future applications in the field of catalytic membranes [15].

The synthesis of Pd catalysts was carried out in ethanol employing microwave (MW) irradiation, a promising less energy-demanding approach compared to conventional heating [16–21]. The Pd/PK-SiO₂ catalysts were tested in two probe reactions: the selective hydrogenation of cinnamaldehyde (CAL) to hydrocinnamaldehyde (HCAL) carried out in decalin and, as a preliminary investigation, in the oxidation of 1-phenylethanol (1-PE) to acetophenone (AcPh) performed in water. The first reaction is a model reaction to investigate the effect of the catalyst morphology on the selectivity [7,9,19,22–28] and, in addition, HCAL has recently been found as an important intermediate for the preparation of pharmaceuticals [25].

The other reaction is important for synthetic organic chemistry [29–36] and water represents the ideal green solvent for industrial applications. In the last decade, several supported metal catalysts were found to be active in the aerobic oxidation of alcohols in water [29,30,32,33]. Among these catalysts, palladium-based ones show promising performances even under mild reaction conditions [35–46], although the number of highly recyclable catalysts working in pure water is still rather limited.

Hereafter, we report the synthesis and characterization of palladium nanoparticle catalysts supported on Aerosil 380, PK and hybrid organic-inorganic PK-SiO₂, in order to investigate the potential of the hybrid systems for catalytic applications.

2. Experimental

2.1. Chemicals

(Pd(OAc)₂), 1,3-bis(diphenylphosphino)propane (dppp) and p-toluenesulfonic acid (TsOH) were purchased from Aldrich and employed as received. [Pd(TsO)(H₂O)(dppp)](TsO) was synthesized as described in the literature [37]. SiO₂ (AEROSIL 380) was purchased from Evonik Industries and employed after treatment under vacuum at 100 °C for 3 h.

The PK support (poly-3-oxotrimethylene) was prepared through CO-ethene copolymerization as described in [38], except for the concentration of the copolymerization catalyst [Pd(TsO)(H₂O)(dppp)](TsO) in MeOH and in the presence of H₂O and TsOH ([Pd] = 0.125 mmol L⁻¹, Pd:H₂O:TsOH = 1:350:10, 85 °C, P 4.5 MPa, CO:ethene = 1:1, 1 h). The PK yield was 6.2 g with an average molecular weight of about 12 kDa. The PK-SiO₂ support was prepared under the same conditions, but in the presence of SiO₂. In the presence of 2 g or 4 g of SiO₂, 8.3 g or 10.1 g of PK-SiO₂ were obtained, respectively. Thus, the presence of SiO₂ does not alter the productivity of the catalytic system. These supports contain 76% and 60% PK and are indicated as 76%PK-SiO₂ and 60%PK-SiO₂, respectively.

All other reagents and standard products were also obtained from Aldrich, purified according to standard procedures [39] and stored under dry argon.

2.2. Preparation of the Pd nanoparticles supported on PK

Table 1 reports the reaction conditions adopted for the preparation of the catalysts and their morphological properties.

The MW-assisted synthesis of Pd catalysts was performed using a CEM Discover S-class oven with a PC control. The apparatus consists of a single-mode, self-tuning cavity where the correct position of the reaction vial is automatically tuned to ensure reproducible conditions at each run. The oven operates with a continuous power generator capable of supplying an irradiation power from 0

to 300 W (with 1 W-step increment) with a fine and automated control of the sample temperature based on the CEM PowerMax technology. The oven allows two different operating ways: at constant temperature (by varying the irradiation power in order to maintain the desired temperature value) or at constant power. The 80 mL glass reactor (Sealed Vessel accessory) was equipped with a magnetic drive stirrer and a vertically-focused IR temperature sensor which provided an accurate temperature control during the process (maximum operating temperature 250 °C). The reactor was also equipped with a pressure line and a pressure probe, the latter allowing the control of the internal pressure throughout each run (maximum operating pressure 1.4 MPa). The selected amount of Pd(OAc)₂ was dissolved in 40 mL EtOH-support suspension under stirring at room temperature. The resulting mixture was MW-irradiated for 10 min at 120 °C under nitrogen atmosphere. The reactor was then rapidly cooled to room temperature, the solvent was removed by filtration under nitrogen and the supported catalysts were washed several times with acetone and ether, dried under vacuum and stored under dry argon.

2.3. Characterization of the catalysts

TEM images of all samples were taken using a Philips CM12 microscope working at 120 kV. Histograms of the particles size distribution were obtained by counting at least 500 particles onto the micrographs. The mean diameter (d_m) was calculated as $d_m = \sum d_i n_i / \sum n_i$ where n_i was the number of particles of diameter d_i . The counting was carried out on electron micrographs obtained starting from 50,000 to 100,000 magnifications, where well-contrasted Pd particles were clearly detected. The graduation of the particle size scale was 0.5 nm.

SEM analyses were carried out using a JEOL JSM 5600 LV working at 200 kV.

NMR experiments were carried out on a Bruker AMX-300WB spectrometer working at 300.13 MHz for proton and at 75.47 MHz for carbon-13 using a 4 mm CP/MAS probe head for solid-state measurements. All experiments were performed at 25 °C.

¹³C cross polarization with magic angle spinning (CP-MAS) NMR spectra were recorded using a contact pulse (t_{CP}) of 1.5 ms with a spin-lock field of 75 kHz, a recycle delay of 10 s and acquiring 6400 scans. The MAS frequency was 9 kHz. Variable contact time CP experiments were performed with t_{CP} values ranging from 100 μs to 80 ms; 400 scans were acquired for each experiment. ¹H-¹³C cross-polarization times (T_{CH}) and ¹H spin-lattice relaxation times in the rotating frame (¹H $T_{1\rho}$) were determined by fitting the peak intensities obtained from variable contact time experiments to the equation [40]:

$$I(t) = \frac{I(0) \exp(-t/T_{1\rho}(H)) - \exp(t/T_{CH})}{1/T_{CH} - 1/T_{1\rho}(H)}.$$

The ¹H spin-spin relaxation times (T_2) were measured from transverse relaxation curves built using the FID following a solid echo sequence ($\pi/2_x - t - \pi/2_y - t$) [41] in order to avoid dead time effects, with a 90° pulse of 3.5 μs and a delay τ of 16 μs. The experiments were performed at resonance on static samples. The FIDs recorded clearly showed two components which could be fitted by a Pake function [42,43] and an exponential one, respectively.

The BET surface area was determined by nitrogen adsorption, using a single point ThermoQuest Surface Area Analyzer Qsurf S1.

The content of Pd was determined by inductively coupled plasma-optical emission spectrometers (ICP-OES) with a Spectro-Genesis instrument equipped with a software Smart Analyzer Vision. For ICP-OES of the solid catalysts, each sample was heated over a heating plate in a porcelain crucible in the presence of aqua

Table 1

Preparation conditions and characterization of different supported Pd catalysts. The syntheses were carried out under MW irradiation at 120 °C for 10 min in 40 mL of EtOH.

Sample	Pd precursor (mg Pd)	Support (g)	Pd (wt%) ^a	Pd: average diameter [Std. dev.] (nm)	Support: average diameter microstructure [Std. dev.] (μm)	BET (m^2/g) ^b	PME ^c %	XPS binding energies Pd 3d _{5/2} (eV)
PD 1	Pd(OAc) ₂ (9.5)	Aerosil 0.70	0.9	17.8 [3.4]	12.2 [4.1]	281	6.3	335.6 (99%) 337.6 (1%)
PD 2	Pd(OAc) ₂ (24.3)	Aerosil 0.70	2.6	19.2 [3.5]	14.7 [5.1]	228	5.8	335.6 (98%) 337.6 (2%)
PD 3	Pd(OAc) ₂ (9.9)	PK 0.70	1.0	8.7 [3.3]	20.8 [5.2]	14	12.9	335.6 (99%) 337.6 (1%)
PD 4	Pd(OAc) ₂ (21.7)	PK 0.71	2.6	10.1 [3.5]	22.4 [5.3]	11	11.1	335.6 (98%) 337.6 (2%)
PD 5	Pd(OAc) ₂ (9.8)	60%PK-SiO ₂ 0.70	1.0	5.2 [2.2]	18.7 [4.0]	128	21.5	335.6 (99%) 337.6 (1%)
PD 6	Pd(OAc) ₂ (24.9)	60%PK-SiO ₂ 0.71	2.8	6.3 [2.4]	19.1 [5.0]	113	17.8	335.6 (98%) 337.6 (2%)
PD 7	Pd(OAc) ₂ (9.8)	76%PK-SiO ₂ 0.70	1.0	5.1 [2.1]	22.0 [7.0]	90	21.9	335.6 (99%) 337.6 (1%)
PD 7 bis	Pd(OAc) ₂ (9.7)	76%PK-SiO ₂ 0.70	1.0	5.0 [2.1]	22.6 [6.9]	90	22.4	335.6 (99%) 337.6 (1%)
PD 8	Pd(OAc) ₂ (24.0)	76%PK-SiO ₂ 0.70	2.5	6.1 [2.5]	24.3 [7.2]	74	18.4	335.6 (98%) 337.6 (2%)

^a Determined by inductively coupled plasma analysis (ICP).

^b Obtained by single point BET.

^c Percentage of metal exposed determined by TEM analysis.

regia (2 mL) for four times, dissolving the solid residue in 0.5 M aqueous HCl. The limit of detection calculated for Pd was 2 ppb.

The X-ray photoelectron spectroscopy analyses were performed with a VGMicrotech ESCA 3000 Multilab spectrometer, using the unmonochromatised Al K α source (1486.6 eV) run at 14 kV and 15 mA. Survey spectra were collected at constant pass energy of 50 eV. Individual peak energy regions were collected at constant pass energy of 20 eV. Samples were mounted on a stub holder using double-sided adhesive tape. In order to avoid the contact with air, the sample mounting was performed inside a glove bag filled with N₂ and then the holder was loaded inside the XPS machine under a N₂ atmosphere. The C 1s peak, set at 285.1 eV, arising from adventitious carbon, was used as reference for the binding energy values. Differential surface charging was ruled out by checking the reproducibility of XPS results in repeated scans under different X-ray exposures. Analyses of the peaks were performed with the software provided by VG, based on non-linear least-square fitting routine using a weighted sum of Lorentzian and Gaussian component curves after background subtraction according to Sherwood [44].

Infrared spectra were collected using a Nicolet FT-IR Nexus spectrometer equipped with a Smart Diffuse Reflectance Accessory.

2.4. Hydrogenation of cinnamaldehyde to hydrocinnamaldehyde

Hydrogenation reactions were carried out in a stainless steel 300 mL mechanically stirred Parr 4560 autoclave equipped with a P.I.D. controller 4843. In each experiment, the proper amount of catalyst, always containing 2.2 mg of palladium, was introduced into the reactor under inert atmosphere. The autoclave was then closed, evacuated up to 65 Pa and a solution of 3.8 mL of cinnamaldehyde in 100 mL of decalin was introduced by suction. The reactor was then pressurized with hydrogen to 2 MPa and heated up to 100 °C, maintaining a stirring speed of 500 rpm, which assured the absence of mass transfer limitations. In order to ascertain the role of mass transfer, the stirring speed was varied from 400 rpm to 1000 rpm adopting the chosen reaction conditions (100 °C, 2 MPa of H₂, 3.8 mL of cinnamaldehyde in 100 mL of decalin) using the catalysts PD 3 and PD 7 (2.2 mg of Pd for every run). The pressure value was held constant at 2 MPa throughout the reaction time. The course of the reaction was monitored by sampling periodically

the liquid through a valve and analyzing it by gas-chromatography. GC analyses were performed with a HP 5890 gas-chromatograph equipped with a HP 3396 integrator, a flame ionization detector and a PONA capillary column (50 m × 0.2 mm × 0.5 μm) with a stationary phase 100% dimethylpolysiloxane (carrier gas nitrogen, flow 1 mL/min).

In every test, it was found that when the stirring speed was greater than 450 rpm further increase of the stirring speed did not affect the catalytic performances, ensuring the absence of external diffusion limitations. Therefore, a stirring speed of 500 rpm was employed.

In order to ascertain the extent of l/s mass-transfer and internal resistances, the following criteria reported by Ramachandran and Chaudhari [45,46] were applied:

Liquid–solid hydrogen-transfer resistance negligible if:

$$\alpha_1 = \frac{R\rho_p d_p}{6k_{1/\text{s}} \text{CwH}_2^*} < 0.1,$$

internal hydrogen resistance negligible if:

$$\alpha_2 = \frac{d_p}{6 \times [\rho_p R / \text{CwD}_{\text{eH}_2} \text{H}_2^*]^{0.5}} < 0.2$$

where R = reaction rate, mol/(m³ s); ρ_p is density of the particle; d_p = average particle diameter, m; k_{1/sH_2} = transfer coefficient of hydrogen from liquid to catalyst, m/s; Cw = catalyst concentration, kg/m³; H_2^* = hydrogen solubility in decalin; D_e (m²/s) is the effective diffusivity of hydrogen in the pores. R is taken as the average reaction rate in the first 30 min for catalyst PD7 (1%Pd/76%PK-SiO₂), which has the biggest particle diameter (22×10^{-6} m) and is the most active, so that the mass transfer resistances are the highest. From the data reported in Table 3, run 4, it is $R = 4.52 \times 10^{-2}$ mol/(m³ s). ρ_p is calculated as (76% ρ_{PK} + 24% ρ_{SiO_2}); bulk density of PK 1240 kg/m³, 2200 kg/m³ for SiO₂ [47]; it is $\rho_p = 1470$ kg/m³.

Due to the small dimensions of the particles, k_{1/sH_2} is calculated by using the relation: $k_{1/\text{sH}_2} = 2D_{\text{H}_2}/d_p$, where D_{H_2} is the diffusivity of hydrogen in decalin. D_{H_2} is calculated by using the relation reported in [45–47]: D_{H_2} (cm²/s) = $7.4 \times 10^{-8} \cdot T(\text{MW}_{\text{decaline}})^{0.5}/(\mu_{\text{decaline}} \cdot V_{\text{H}_2})^{0.6}$ where $\text{MW}_{\text{decaline}}$ = molecular weight of decalin; μ_{decaline} = viscosity

of decalin, taken as 0.1 cP, by extrapolating the data reported in [48] at 373 K, the reaction temperature; V_{H_2} = molar volume of hydrogen at the normal boiling point, 7.03 cm³/mol [47]. It is $D_{\text{H}_2} = 1.1 \times 10^{-7}$ m²/s and $k_{1/\text{SH}_2} = 1.0 \times 10^{-2}$ m/s. $D_{e\text{H}_2}$ can be safely taken as $D_{\text{H}_2}/5 = 0.22$ m²/s [51]. It is $C_w = 2.2$ kg/m³, $H_2^* = 66$ mol/m³, calculated at 373 K, under 2 MPa from [49]. Using these data, it is $\alpha_1 = 1.67 \times 10^{-4} \ll 0.1$ and $\alpha_2 = 1.66 \times 10^{-2} < 0.2$, therefore the external and internal resistances are negligible. These parameters are even smaller because the actual ρ_p is <1470 kg/m³, due to the porosity of the particles. The same conclusions can be drawn with the other catalysts, which are less active and have smaller particle size, or also if one takes into consideration the resistances of CAL transfer. In the above relations it is enough to substitute D_{H_2} and $D_{e\text{H}_2}$ with D_{CAL} and $D_{e\text{CAL}}$, H_2^* with the concentration of CAL in mol/m³ and V_{H_2} with V_{CAL} at the normal boiling point.

The reproducibility of repeated catalytic runs was within 5%. Recycling experiments were carried out by removing the liquid reaction mixture through the sample valve, evacuating the autoclave and then charging again with the fresh CAL solution for the subsequent catalytic run. Leaching tests were carried out as follows: at the end of the first hydrogenation run the solid catalyst was filtered off under inert atmosphere and the recovered solution was reused for a second hydrogenation.

Activity was calculated as converted moles of CAL per mole of Pd in the whole catalyst per second, measured after 30 min of reaction and at 100 mol% CAL conversion. TOF numbers (turnover frequencies) after 30 min of reaction were calculated as moles of converted cinnamaldehyde per mole of exposed Pd per second. The amount of exposed Pd was calculated on the basis of percentage of metal exposed (PME) estimated from the expression $\text{PME} = 112/d(\text{nm})$ assuming spherical particles for Pd [50].

2.5. Oxidation of 1-phenylethanol to acetophenone

Oxidation reactions and recycling and leaching experiments were carried out using the same apparatus and procedures adopted for the hydrogenation reaction. Reaction conditions are reported in Table 5. GC analyses were performed using the same instrument and conditions reported in the previous section. The reproducibility of the catalytic runs was within 5%.

3. Results and discussion

3.1. Catalyst characterization

3.1.1. Characterization of the supports

The features of the supports used for the preparation of the Pd catalysts are reported in Table 2.

The infrared spectra of Aerosil 380, of the hybrid 60%PK-SiO₂ and of the PK powders are shown in Fig. 1.

The infrared spectrum of the hybrid 60%PK-SiO₂ is essentially the superposition of SiO₂ and PK spectra. The presence of the OH stretching modes of hydroxyl groups in the spectra of both pristine SiO₂ and the PK-SiO₂ material between 3800 and 3000 cm⁻¹ indicates that there are not chemical bonds between the PK and the OH groups present on the surface of silica nanoparticles.

The surface areas of the different supports (SiO₂, 60%PK-SiO₂, 76%PK-SiO₂ and bare PK) were measured using a single point BET equation and resulted 306, 140, 117 and 16 m²/g, respectively. The decreasing values of the surface area of the hybrid materials with increasing % of PK are in line with the much lower contribution of the PK to the surface area.

¹³C CP-MAS NMR spectra of PK with and without SiO₂ do not show differences, all spectra displaying only the signals at 35.5 and

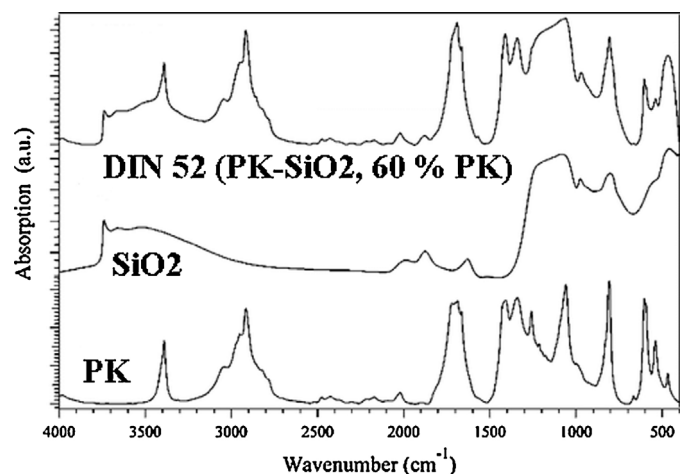


Fig. 1. Infrared spectra of pristine PK, SiO₂ and 60%PK-SiO₂ in the region from 4000 to 400 cm⁻¹.

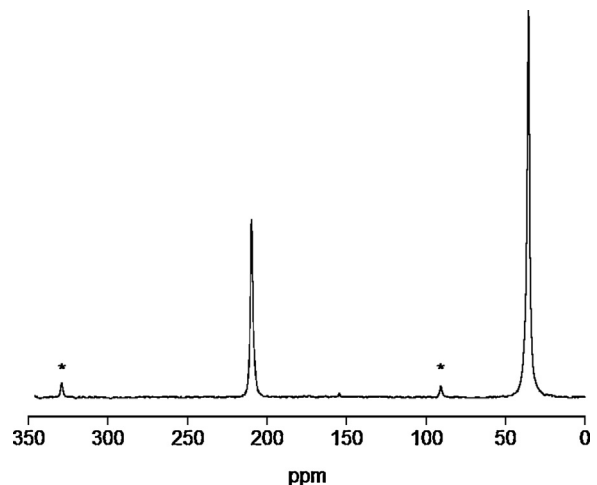


Fig. 2. ¹³C CPMAS NMR spectrum of PK (asterisks indicate spinning side bands).

209.9 ppm ascribable to methylene and carbonyl carbons, respectively. Variable contact time CP experiments reveal that the only difference between the different samples was in the ¹H $T_{1\rho}$ values, which were 42 ± 2 ms for PK and 50 ± 2 for 76%PK-SiO₂ and 60%PK-SiO₂, thus showing a slightly higher rigidity for PK. In order to better highlight differences in the degree of crystallinity, ¹H FID analysis was performed. The FIDs were well fitted with a Pake and an exponential contribution, the former ascribable to a crystalline component, the latter to an amorphous one. The results of the fitting indicated that the crystalline contribution is higher for PK, i.e. 84% of the ¹H signal compared to 80% and 78% in the case of 76%PK-SiO₂ and 60%PK-SiO₂, respectively (see Table 2). Furthermore, the amorphous component in PK is characterized by a T_2 value of 410 ± 10 μ s compared to a value of 122 ± 20 μ s determined for 60%PK-SiO₂ indicating a more rigid amorphous phase in the latter sample. These results suggest that the presence of SiO₂ induces a change in polymer morphology, causing a decrease in crystalline component accompanied by a decrease in mobility of the amorphous one.

Fig. 2 shows the ¹³C CPMAS NMR spectrum of PK, whereas Fig. 3 reports ¹H FID of PK (solid line) and of 60%PK-SiO₂ (dashed line).

SEM analyses show their macro-structures where aggregated particles are evidenced. The average diameters of macro-structures of bare silica aggregates, bare PK, 60%PK-SiO₂, 76%PK-SiO₂ are 20.7, 6.9, 7.1 and 7.0 μ m, respectively. The structure of Aerosil was also

Table 2

Characterization of the employed supports.

Support	% PK	BET (m^2/g) ^a	% PK crystallinity ^b	Average diameter of macrostructure [Std. dev.] (μm)
Aerosil	0	306	–	20.7 [9.2]
PK	100	16	84	6.9 [1.5]
60%PK-SiO ₂	60	140	78	7.1 [2.1]
76%PK-SiO ₂	76	117	80	7.0 [2.2]

^a Obtained by single point BET.^b Crystallinity of the PK component determined by NMR.

investigated using TEM technique, which allowed us to detect its primary nanoparticles having an average diameter of 13.3 nm with a standard deviation of 4.2. The pore size characterization (see Supplementary Information) evidenced that the deposition of PK over silica support leads to a total disappearance of the original silica microporosity.

3.1.2. Characterization of the catalysts

All these supports were used for the synthesis of Pd catalysts, whose features are reported in Table 1. The Pd average particle diameter of samples supported on silica PD 1 and PD 2, with 0.9 and 2.6 wt% Pd, are 17.8 and 19.2 nm, with standard deviations of 3.4 and 3.5, respectively. Fig. 4A shows the TEM image and the particle size distribution for PD 1.

The surface areas of PD 1 and PD 2 are 281 and 228 m^2/g , respectively (Table 1), smaller if compared to that of the pristine SiO₂, which suggests that standard pre-treatments carried out on SiO₂ before its employment as support, the successive Pd deposition and the final catalyst work-up partially aggregate the SiO₂ particles. These samples were also characterized by XPS analysis. In Table 1 the binding energies relative to Pd 3d_{5/2} photoelectron transition characterized by two components, respectively at 335.6 and 337.6 eV, are reported. The low binding energy component at 335.6 eV is attributed to metallic Pd(0), whereas the high energy component at 337.6 eV is due to oxidized Pd²⁺ [51].

PD 1 and PD 2 samples show an almost complete Pd reduction, as evidenced by the 99% and 98% abundance of the peak at 335.6 eV.

On the other hand, PD 3 and PD 4 were synthesized employing the bare PK as support, with analogous Pd loading, 1 and 2.6 wt%, respectively. The introduction of palladium causes a lowering of surface area compared to the bare support, as expected. TEM analysis shows a Pd particle size distribution with average diameters of 8.7 and 10.1 nm and standard deviations of 3.3 and 3.5 respectively. In Fig. 4B the TEM image and the particle size distribution of sample PD 3 are reported, where it is also possible to observe the presence of some Pd aggregates. On the PK Pd particles are smaller than those supported on silica. The higher stabilizing ability of PK may be due not only to steric but also to electronic effects through the interactions of its keto groups with Pd nanoparticles.

SEM and TEM analyses show that the texture of the PK before and after the deposition of palladium is similar (Fig. 5).

Again, the complete reduction of Pd was again ascertained by XPS spectroscopy (Table 1).

Samples PD 5 and PD 6 were synthesized in similar manner as the previous ones, with a 1 and 2.8 wt% Pd loading, respectively, but using the hybrid 60%PK-SiO₂ material as support. Both catalysts are characterized by much smaller palladium nanoparticles with a more homogeneous particle size distribution, average diameters of 5.2 and 6.3 nm and standard deviations of 2.2 and 2.4, respectively. Fig. 6A shows the TEM image and the particle size distribution for sample PD 5. On the PK-SiO₂ supports the Pd nanoparticles result significantly smaller with a more homogeneous size distribution compared to those on bare SiO₂ or PK. This suggests that for the hybrid supports the stabilizing role of the prevailing PK component is preserved and rather enhanced by the increase of surface area resulting in lower probability of metal particles to be closed to other ones and aggregate.

Also in this case, XPS analysis evidenced that both catalysts present an almost complete Pd reduction. Samples PD 7 and PD 8, prepared using the hybrid support with 76% of PK, show Pd nanoparticles with dimensions similar to those of the previous hybrid catalysts, characterized by average diameters of 5.1 and 6.1 nm and standard deviations of 2.1 and 2.5 respectively. Fig. 6B shows TEM image and particle size distribution for sample PD 7. BET surface areas for these samples resulted of 90 and 74 m^2/g , lower than those of the corresponding catalysts supported on 60%PK-SiO₂. Again, XPS analysis confirms the complete Pd reduction.

When both hybrid supports were used, the pore size characterization (see Supplementary Information) reveals that the deposition of palladium increases the disappearance of the original silica microporosity, as already observed before the introduction of Pd in the composite material respect to the pristine SiO₂.

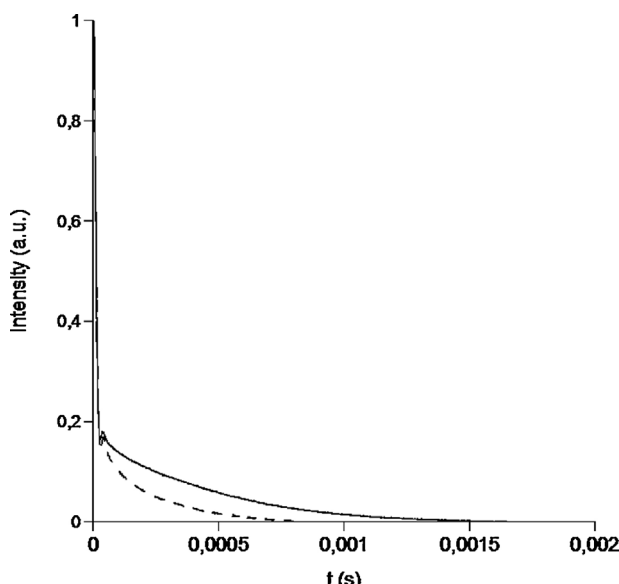


Fig. 3. ¹H FID of PK (solid line) and of 60%PK-SiO₂ (dashed line).

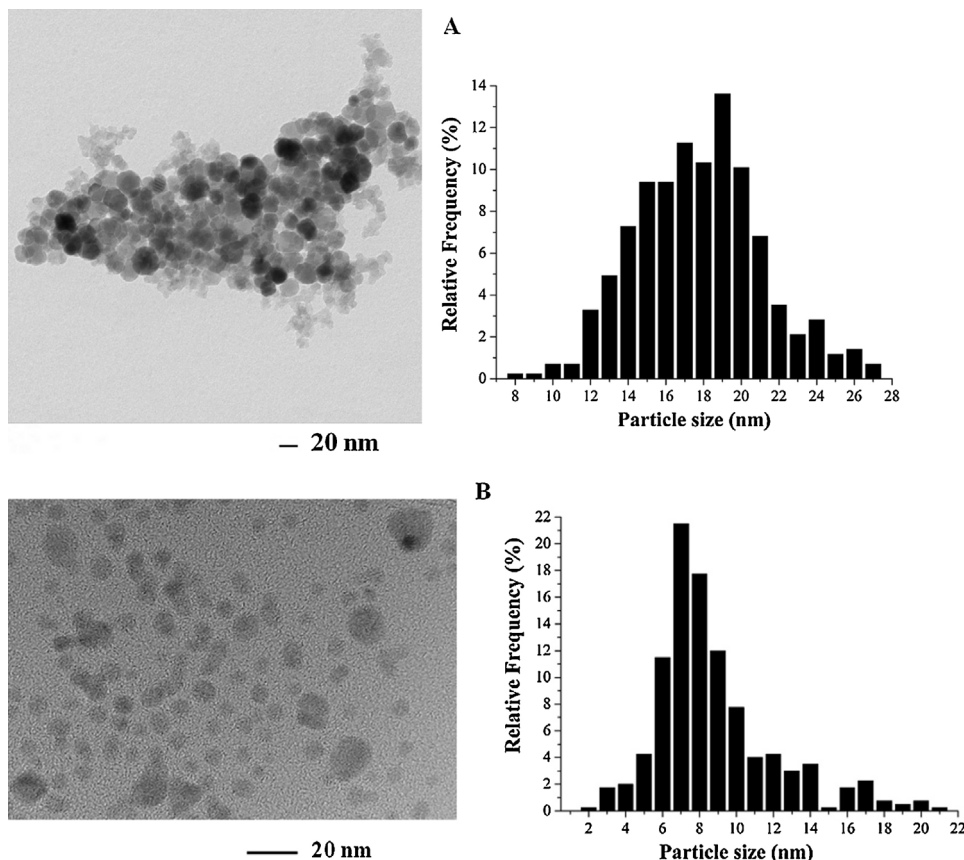


Fig. 4. TEM images and particle size distributions of samples PD 1 (A) and PD 3 (B).

The synthesis of sample PD 7 was duplicated (sample PD 7 bis, **Table 1**): TEM, XPS and BET analysis show that the preparation under MW irradiation is highly reproducible (**Table 1**).

3.2. Catalytic tests

As reported in the experimental section, the employed PK was prepared by CO-ethene copolymerization catalyzed by a Pd(II) complex, with the risk of contamination by trace amounts of palladium. Therefore, preliminary blank hydrogenation of CAL and oxidation of 1-PE tests were carried out using the bare PK under typical reaction conditions reported in **Tables 3 and 5**: no reaction occurred, thus any contribution to the catalytic activity from traces of palladium employed in the copolymerization can be excluded.

3.2.1. Hydrogenation of CAL

The supported Pd catalysts were tested in the hydrogenation of CAL to HCAL adopting the reaction conditions reported in **Table 3**. **Scheme 1** shows the possible hydrogenations of the different functional groups, C=C and C=O double bonds.

It is remarkable that in each case the only ascertained by-product was 3-phenyl-1-propanol (HCOL), whereas cinnamyl alcohol (COL) was detected only in trace amounts.

The result obtained testing the sample PD 3 and PD 4 supported on pure PK is in line with our previous results where Pd was supported on a PK of higher molecular weight (>50 kDa) [9]. In the present study, we preferred to use a PK of 12 kDa prepared according to the conditions reported in the experimental section, since the yield in the hybrid PK-SiO₂ was more easily reproducible when the synthesis was repeated in the presence of SiO₂, then when

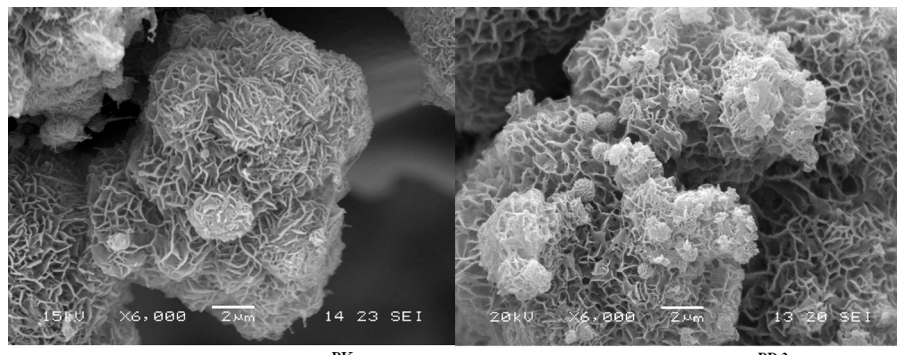


Fig. 5. SEM image comparison between PK and PD 3.

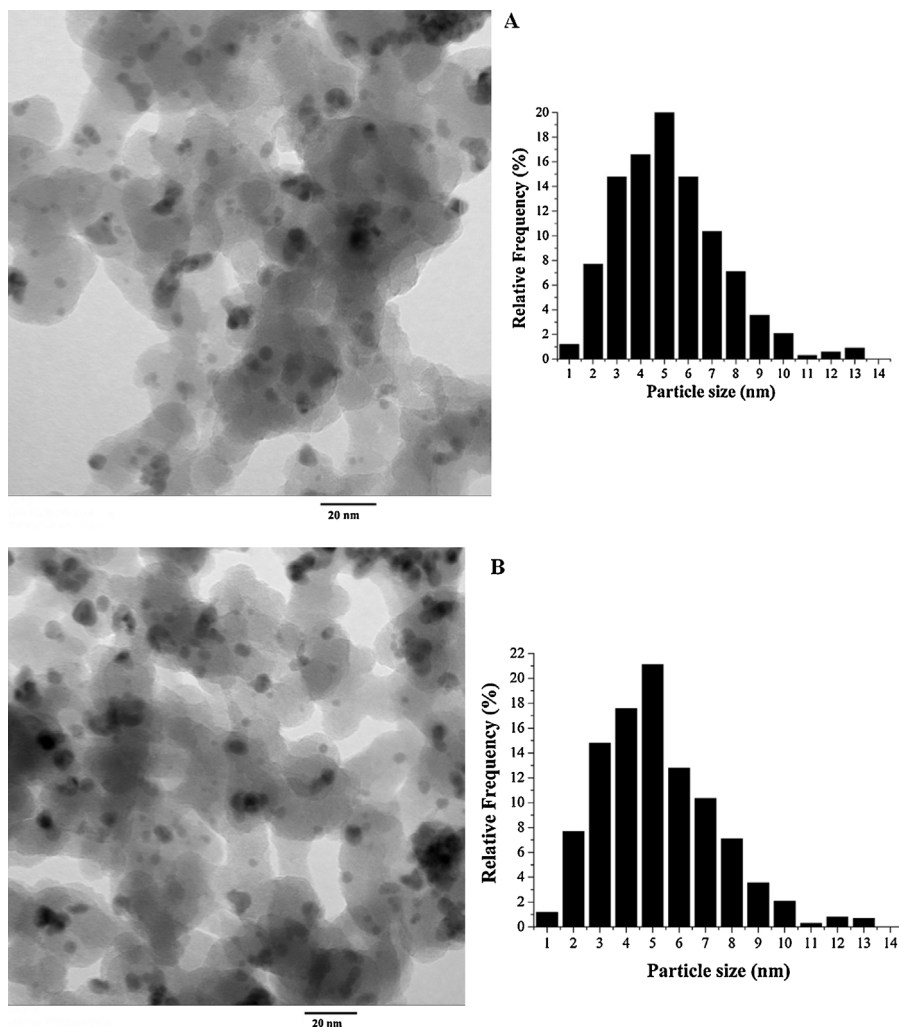
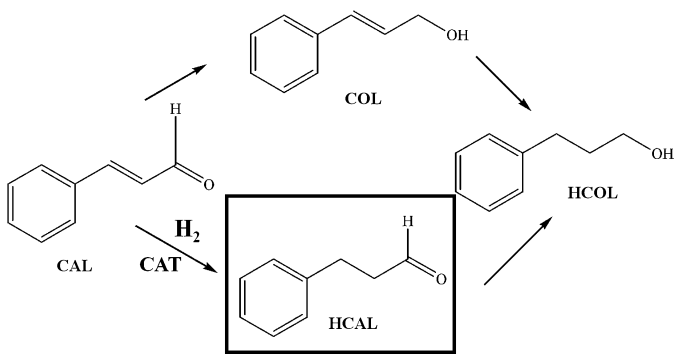


Fig. 6. TEM images and particle size distributions of samples PD 5 (A) and PD 7 (B).



Scheme 1. Reaction pathway of the hydrogenation of cinnamaldehyde.

using the conditions described in [9]. For each couple of catalysts on the same support, the most active and selective to HCAL are those with lower Pd loading, characterized by smaller palladium particle sizes, as found for other palladium catalysts employed in the same reaction [9,52,53]. The particle size effect was attributed to the position of cinnamaldehyde molecule respect to the metal surface. The surface of small particles was assimilated to a curved surface, whereas the surface of big particles was seen as a flat surface which leads to an enhanced repulsion between the phenyl ring

and the metal nanoparticle. Consequently, in the second case, the distance between C=C bond and the catalyst is increased, causing a lower selectivity towards the C=C bond hydrogenation, as well evidenced by Chizari et al. [54]. In effect, in our study, the highest selectivity to HCAL was obtained in run 5 carried out with PD 7 (1.0% Pd/76%PK-SiO₂), characterized by the smallest Pd particle size and narrowest size distribution.

A further inspection of the results reported in Table 3 shows that the activity based on Pd in the whole catalyst is in the order Pd/PK-SiO₂ > Pd/SiO₂ > Pd/PK for both Pd loadings, even though the surface area follows the order Pd/SiO₂ > Pd/PK-SiO₂ >> Pd/PK.

The recovery and reusability of the catalysts was investigated by recycling samples PD 7 and PD 1 five times. The results shown in Fig. 7 and Table 3 highlight that no loss of activity and selectivity occurs with sample PD 7, whereas for sample PD 1 there is a marked decrease both in activity and selectivity.

These results can be ascribed to the aggregation of Pd particles ascertained for PD 1 after the catalytic runs, as revealed by TEM analyses (Table 4) of the sample recovered after five catalytic cycles (run 10, Table 3).

On the contrary, after the catalytic run 9, sample PD 7 reveals unchanged morphology at TEM analysis. The progressive decrease of activity shown by PD 1 can be also ascribed to the leaching of Pd from the solid catalyst. In fact, the Pd loading of PD 1 after five cycles was decreased to 0.7 wt%, whereas for PD 7 remained unchanged at

Table 3

Catalytic performances of supported Pd catalysts in the hydrogenation of cinnamaldehyde to hydrocinnamaldehyde.

Run ^a	Sample description	Conv. (mol%) after 30 min	$A_{30\text{min}}^b$ (mol (mol Pd s) $^{-1}$)	$A_{100\%}^c$ (mol (mol Pd s) $^{-1}$)	Sel. to HCAL at 100 mol% conversion (mol%)	TOF ^d (s $^{-1}$)
Blank test	PK	–	–	–	–	–
1	Sample PD 1 0.9 wt% Pd/Aerosil	56.1	0.46	0.10	72.8	7.2
2	Sample PD 2 2.6 wt% Pd/Aerosil	18.2	0.15	0.05	71.6	2.5
3	Sample PD 5 1.0 wt% Pd/60%PK-SiO ₂	93.3	0.76	0.41	80.2	3.5
4	Sample PD 6 2.8 wt% Pd/60%PK-SiO ₂	51.4	0.42	0.14	78.4	2.3
5	Sample PD 7 1.0 wt% Pd/76%PK-SiO ₂	98.0	0.79	0.41	82.4	3.6
6	Sample PD 8 2.5 wt% Pd/76%PK- -SiO ₂	22.2	0.18	0.08	78.3	1.0
7	Sample PD 3 1.0 wt% Pd/PK	30.6	0.25	0.04	76.8	1.9
8	Sample PD 4 2.6 wt% Pd/PK	23.0	0.19	0.03	75.9	1.7
9	Sample PD 7 recovered after 5 catalytic cycles	94.4	0.76	0.32	82.0	3.5
10	Sample PD 1 recovered after 5 catalytic cycles	35.0	0.28	0.07	60.5	5.0

^a Reaction conditions: 100 °C, 2 MPa of H₂, 2.2 mg of Pd, 3.8 mL of cinnamaldehyde in 100 mL of decalin as solvent.^b Activity measured at 30 min of reaction as converted moles of CAL per mole of Pd in the whole catalyst per second.^c Activity measured at 100 mol% CAL conversion.^d TOF (turnover frequency) after 30 min of reaction, calculated as moles of converted cinnamaldehyde per mole of exposed Pd per second.

1.0 wt%. In order to exclude any metal leaching from the supported Pd systems (which could lead to highly active soluble Pd species), the solution recovered by filtration after the catalytic run 5 of sample PD 7 was tested in the hydrogenation of CAL. No further catalytic activity was ascertained. Moreover, the presence of palladium in the reaction mixture was excluded by ICP-OES, thus confirming the stability of the Pd/PK-SiO₂ heterogeneous catalysts. In our previous paper we had yet underlined the stability and recyclability of Pd/PK systems [9]. The above results evidence that PK present on the hybrid support is still able to play a significant stabilizing effect for Pd species also during catalysis, not exerted by bare silica. The Pd catalysts supported on the hybrid systems generally show higher metal dispersions and TOF values than the corresponding systems supported on bare PK (see Table 3), the increase of surface area of the hybrid supports resulting in lower probability of Pd particles

to aggregate. The high TOF values determined for Pd/SiO₂ could be scarcely reliable due to the ascertained contribution of leached palladium species to the catalytic performance.

In general, it is difficult to compare the obtained results (in terms of activity and TOF values) with those reported in the literature, due to the different adopted conditions (pressure, temperature, duration, solvent) and lacking of information on Pd particles dimensions for many systems. In a previous work of our group, Pd catalysts anchored on a cross-linked styrene/divinylbenzene resin functionalized with bis(diphenylphosphino)methane ligands were used for the hydrogenation of CAL in decalin adopting reaction conditions similar to those of the present paper. After 30 min of reaction, an activity of about 0.43 converted moles of CAL per mole of Pd in the whole catalyst per second was achieved [7]. An activity value up to 0.79 after 30 min has been reached using the catalyst PD7.

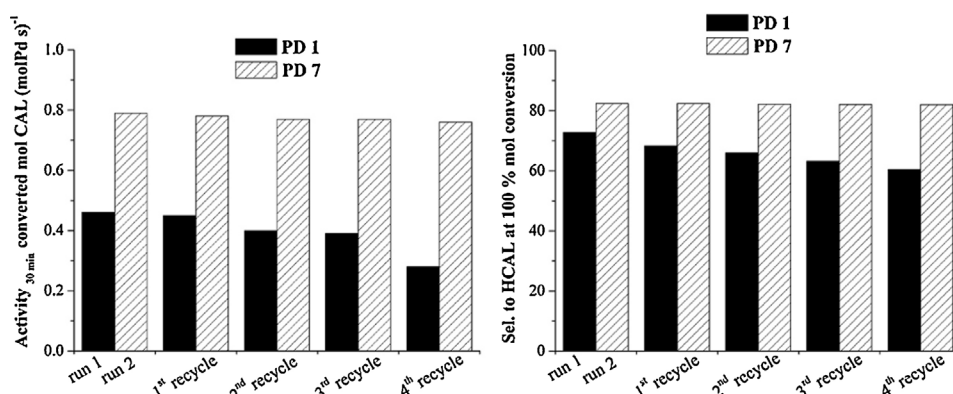
**Fig. 7.** Activity_{30min} and selectivity to HCAL at 100 mol% CAL conversion in the hydrogenation of CAL in the presence of samples PD 1 and PD 7 carried out at 100 °C, 2 MPa of H₂ using 2.2 mg of Pd, 3.8 mL of cinnamaldehyde in 100 mL of decalin (first hydrogenation runs, runs 1 and 5 respectively and successive recycles of the solid catalysts).

Table 4

Averages diameters, standard deviations and percentage of metal exposed (PME) of samples PD 7 and PD 1 after their employment in catalytic runs 9 and 15 (PD 7) and 10 and 16 (PD 1).

Sample	Average diameter [Std. dev.] (nm)		PME ^a
Catalysts used for 5 cycles in the hydrogenation of CAL			
Recovered sample PD 7	5.1	[2.2]	22.0
1.0 wt% Pd/76%PK–SiO ₂			
Recovered sample PD 1	19.8	[4.2]	5.7
0.9 wt% Pd/Aerosil			
Catalysts used for 5 cycles in the oxidation of 1-PE			
Recovered sample PD 7	5.2	[2.2]	21.5
1.0 wt% Pd/76%PK–SiO ₂			
Recovered sample PD 1	19.4	[4.1]	5.8
0.9 wt% Pd/Aerosil			

^a Percentage of metal exposed determined by TEM analysis.

On the other hand, when a 5% Pd/C catalyst was adopted for the hydrogenation of CAL in decalin under mild conditions (30 °C and 0.1 MPa of hydrogen), hydrocinnamaldehyde was produced with a very low selectivity, 33.6%, at complete CAL conversion. Moreover, no mention of the recyclability of the catalysts was made [22].

A very recent paper reports an interesting comparison of TOF data for CAL hydrogenation employing different Pd supported catalysts (Pd/C, Pd/carbon nanofiber, Pd/carbon nanofiber/TiO₂, Pd/Al₂O₃, Pd/SiO₂) in the temperature range of 60–80 °C and pressure range of 0.2–4 MPa of hydrogen, in different solvents [23]. The reported TOF values are within the range 0.16–6.7 s⁻¹ and for Pd/SiO₂ up to 3.4 s⁻¹, but in this last case the selectivity to HCAL at complete conversion of the substrate is always lower than 60%.

Finally, in a very recent paper of Fujiwara, Pd/SiO₂ in water at 25 °C and 0.1 MPa of hydrogen allowed to reach a conversion value after 4 h of reaction of only 23% with a selectivity to HCAL of 87%, corresponding to a TOF of 0.004 s⁻¹. When novel Pd nanoparticles supported on boronate polymers were adopted, 90% yield was ascertained at complete conversion, with a TOF of 0.019 s⁻¹, a value significantly low. Moreover, the preparation of this catalyst required a complex multi-step synthetic procedure [24].

On the base of the above discussion, the reached results, in terms of TOF values and recyclability, are comparable, in terms of TOF values and recyclability, with the leading results up to now reported.

3.2.2. Oxidation of 1-PE

Pd catalysts which showed the most promising performances in the hydrogenation of CAL (i.e. samples PD 1, 3, 5 and 7) were also tested in a preliminary study on the oxidation of 1-PE to AcPh in water (**Scheme 2**).

The catalytic performances are reported in **Table 5**. All the reactions are completely selective to ketone, no other by-products were detected in the reaction mixture also when complete conversion was reached (run 12, **Table 5**), in particular benzaldehyde and benzoic acid, well known by-products of this reaction, were absent [55].

In the case of PD 1 supported on SiO₂, the yields in acetophenone are 44.9 and 75.1 mol% after 6 and 12 h of reaction, respectively. Sample PD 3, where Pd is supported on the bare PK, gives the poorest results. More promising outcomes are achieved with samples PD 7 and PD 5 supported on the hybrid material SiO₂–PK, reaching yields of 58.3 and 62.2 mol% after 6 h of reaction and 94.8 and 100 mol% after 12 h respectively. These results can be related to the different affinity among the catalyst surface, the substrate, the oxidation product and the solvent. In fact, according to Prati et al. [33,56,57], the performance in the oxidation of hydrophobic and hydrophilic alcohols in the presence of Pd catalysts supported on carbon nanotubes, whose surface was modified in order to change the hydrophobic/hydrophilic properties, was different in polar or

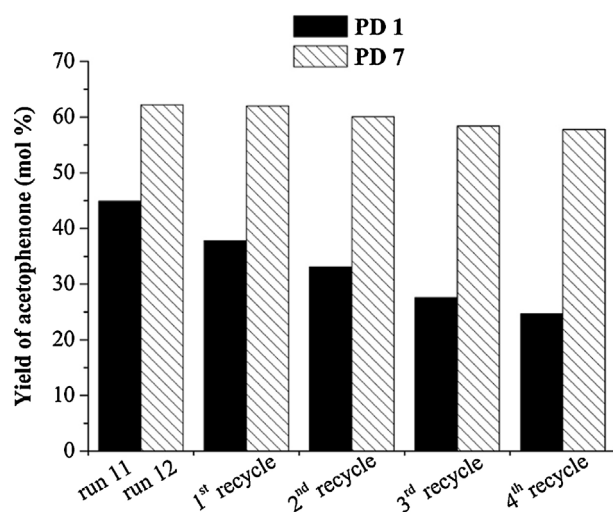
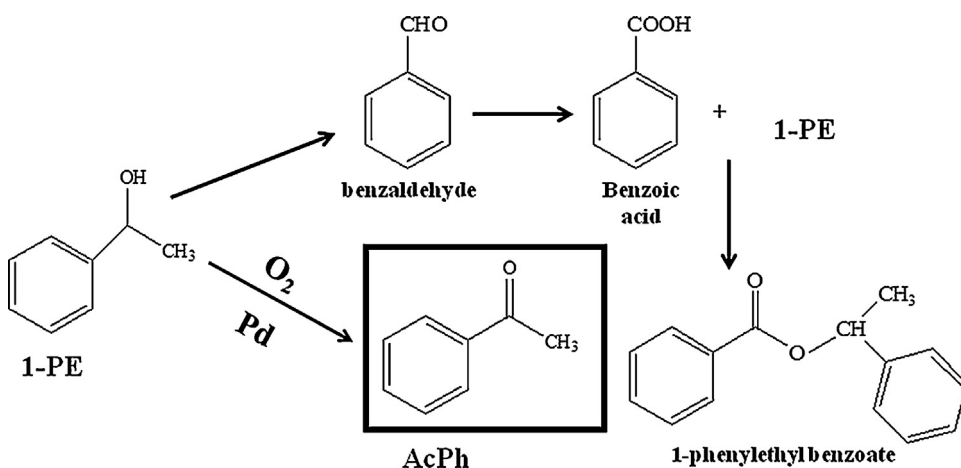


Fig. 8. Yield of acetophenone (mol%) in the oxidation of 1-PE after 6 h of reaction in the presence of samples PD 1 and PD 7 carried out at 100 °C, 1 MPa of O₂ using 1.0 mg of Pd, 300 mg of 1-phenylethanol in 5 mL of water (first hydrogenation runs, runs 11 and 12 respectively and successive recycles of the solid catalysts).

apolar solvent. In particular, they studied the oxidation of benzyl alcohol in cyclohexane and in water at 100 °C under 0.2 MPa of oxygen in the presence of Pd catalysts supported on functionalized carbon nanotubes (CNTs). In cyclohexane the performances of modified Pd/CNTs catalysts followed their hydrophobic properties, being the most hydrophilic support worst, while in water the behaviour of the most hydrophilic catalyst considerably increased. The beneficial effect of water was explained taking into account that in this medium the catalyst with the most hydrophilic surface could take the highest advantage for the surface–solvent contact, due to their high affinity. This effect was also ascertained in the aerobic oxidation of several alcohols (benzyllic, 1-phenylethanol etc.) in water under atmospheric pressure of O₂ employing palladium nanoparticles supported on a new ordered mesoporous silica with cage-like structure. In particular, in the oxidation of 1-phenylethanol, a conversion of 96.9% with selectivity more than 99% to acetophenone was reached, working at 50 °C for 10 h. The catalysts showed good recyclability and it is possible to address this behaviour to the particular ordered structure of the support which, however, requires a complex multi-step preparation [34]. Our results are in line with those just mentioned: the presence of hydrophilic SiO₂ in the hybrid support favours the activation of 1-PE on catalyst surface. This effect may explain the higher yields achieved when employing catalysts PD 7 and PD 5 compared to that obtained with PD 3. The yields in the case of PD 7 and PD 5 are even better than that of PD 1 and this may be ascribed to the better stabilizing effect of PK towards Pd NPs in comparison with the pristine SiO₂. This was also evidenced by recycle tests, an aspect that represents one of the main criticisms for Pd catalyzed oxidation of alcohols in water. Samples PD 7 and PD 1 were recycled five times under the same reaction conditions (**Fig. 8** and **Table 5**).

Sample PD 7 maintained its initial performance, whereas with sample PD 1 a marked decrease was observed. This last result is ascribable to the aggregation of Pd particle after the catalytic run, as shown by TEM analysis of samples PD 7 and PD 1 after use (see **Table 4**), which again confirms the capacity of the PK component to act as a stabilizer. The significant aggregation on bare silica has been already observed for other Pd nanocatalysts [34].

In order to exclude metal leaching from the supported Pd systems leading to highly active soluble Pd species, the solution recovered by filtration after the catalytic run 13 of sample PD 7

**Scheme 2.** Reaction pathway for the oxidation of 1-phenylethanol.**Table 5**

Catalytic performances of supported Pd catalysts in the oxidation of 1-phenylethanol to acetophenone after 6 and 12 h of reaction.

Run ^a	Sample description	Yield of acetophenone (mol%) after 6 h	Selectivity to acetophenone	Yield of acetophenone (mol%) after 12 h	Selectivity to acetophenone
Blank test	PK	—	—	—	—
11	Sample PD 1 0.9 wt% Pd/Aerosil	44.9	100	75.1	100
12	Sample PD 5 1.0 wt% Pd/60%PK-SiO ₂	62.2	100	100	100
13	Sample PD 7 1.0 wt% Pd/76%PK-SiO ₂	58.3	100	94.8	100
14	Sample PD 3 1.0 wt% Pd/PK	30.1	100	61.6	100
15	Sample PD 7 recovered after 5 catalytic cycles	57.8	100	93.6	100
16	Sample PD 1 recovered after 5 catalytic cycles	24.7	100	41.3	100

^a Reaction conditions: 100 °C, 1 MPa of O_2 , 1.0 mg of Pd, 300 mg of 1-phenylethanol in 5 mL of water as solvent.

was tested in the oxidation of 1-PE. Neither further catalytic activity of the liquid phase nor the formation of palladium black were ascertained, thus confirming the effective stabilizing capacity of the PK in the hybrid PK-SiO₂.

4. Conclusions

The organic-inorganic hybrid material PK-SiO₂ has been employed for the first time as support and stabilizer for Pd nanoparticles. The prepared Pd catalysts, synthesized in ethanol adopting MW irradiation, were morphologically characterized and tested in the hydrogenation of CAL to HCAL and in the oxidation of 1-PE to AcPh. In both reactions they revealed higher activity in comparison with the corresponding systems supported on the bare PK or SiO₂ and excellent recyclability without metal leaching. These results, due to the combined properties of the hybrid support, were ascertained in very different polarity media. In the hydrogenation reaction carried out in decalin, the beneficial effect of SiO₂ on the increase of the surface area combines with the capacity of PK to stabilize the palladium nanoparticles, preventing not only their growth during the catalytic reactions but also their leaching into solution. On the other side, in polar media, such as water, the stabilizing effect of PK is combined with the presence of hydrophilic SiO₂, which induces a better compatibility among the catalyst surface, the reaction medium and the substrate. The oxidation of 1-PE to AcPh evidenced total selectivity to ketone also at complete

conversion of the substrate, and the recyclability of the catalyst for five cycles without metal leaching was again ascertained.

Appendix A. Supplementary data

Supplementary material related to this article can be found, in the online version, at <http://dx.doi.org/10.1016/j.apcata.2015.01.045>.

References

- [1] N.V. Long, C.M. Thi, M. Nogami, M. Ohtaki, Recent Pat. Mater. Sci. 5 (2012) 175–190.
- [2] R.G. Chaudhuri, S. Paria, Chem. Rev. 112 (2012) 2373–2433.
- [3] M.R. Jones, K.D. Osberg, R.J. Macfarlane, M.R. Langille, C.A. Mirkin, Chem. Rev. 111 (2011) 3736–3827.
- [4] S.B. Yin, S.C. Mu, H.F. Lv, N.A.C. Cheng, M. Pan, Z.Y. Fu, Appl. Catal. B: Environ. 93 (2010) 233–240.
- [5] K. Strzelecki, K. Wąsikowska, M. Cypryk, P. Pospiech, e-Polymers 024 (2011) 1–12.
- [6] K. Zhan, H. You, W. Liu, J. Lu, P. Lu, J. Dong, React. Funct. Polym. 71 (2011) 756–765.
- [7] F. Benvenuti, C. Carlini, M. Marchionna, A.M. Raspolli Galletti, G. Sbrana, J. Mol. Catal. A: Chem. 145 (1999) 221–228.
- [8] I. Favier, D. Picurelli, C. Pradel, J. Durand, B. Milani, M. Gomez, Inorg. Chem. Commun. 13 (2010) 766–768.
- [9] A.M. Raspolli Galletti, L. Toniolo, C. Antonetti, C. Evangelisti, C. Forte, G. Martra, M. Manzoli, Appl. Catal. A: Gen. 447–448 (2012) 49–59.
- [10] A. Molazemhosseini, H. Tourani, M.R. Naimi-Jamal, A. Khavandi, Polym. Test. 32 (2013) 525–534.
- [11] A. Molazemhosseini, H. Tourani, A. Khavandi, B. Eftekhari Yekta, Wear 303 (2013) 397–404.

- [12] C.J. Chen, H.T. Lu, W.Y. Tseng, I.H. Tseng, S.L. Huang, M.H. Tsai, *J. Appl. Polym. Sci.* 122 (2011) 648–656.
- [13] G. Zhang, L. Chang, A.K. Schlarb, *Compos. Sci. Technol.* 69 (2009) 1029–1035.
- [14] V. Di Noto, M. Piga, G.A. Giffin, M. Schuster, G. Cavinato, L. Toniolo, S. Polizzi, *Chem. Mater.* 23 (2011) 4452–4458.
- [15] F. Liguori, P. Barbaro, C. Giordano, H. Sawa, *Appl. Catal. A: Gen.* 459 (2013) 81–88.
- [16] A.M. Raspolli Galletti, C. Antonetti, M. Bertoldo, F. Piccinelli, *Appl. Catal. A: Gen.* 468 (2013) 95–101.
- [17] A.M. Raspolli Galletti, C. Antonetti, M. Marracci, F. Piccinelli, B. Tellini, *Appl. Surf. Sci.* 280 (2013) 610–618.
- [18] C. Antonetti, M. Oubenali, A.M. Raspolli Galletti, P. Serp, G. Vannucci, *Appl. Catal. A: Gen.* 421 (2012) 99–107.
- [19] A.M. Raspolli Galletti, C. Antonetti, A.M. Venezia, G. Giambastiani, *Appl. Catal. A: Gen.* 386 (2010) 124–131.
- [20] C. Antonetti, A.M. Raspolli Galletti, I. Longo, *Int. J. Chem. React. Eng.* 8 (2010) 1–17.
- [21] A.M. Raspolli Galletti, C. Antonetti, I. Longo, G. Capannelli, A.M. Venezia, *Appl. Catal. A: Gen.* 350 (2008) 46–52.
- [22] L. Zhang, J.M. Winterbottom, A.P. Boyes, S. Raymahasay, *J. Chem. Technol. Biotechnol.* 72 (1998) 264–272.
- [23] T. Szumelda, A. Drelinkiewicz, R. Kosydar, J. Gurgul, *Appl. Catal. A: Gen.* 487 (2014) 1–15.
- [24] S. Fujiwara, N. Takanashi, R. Nishiyabu, Y. Kubo, *Green Chem.* 16 (2014) 3230–3236.
- [25] S. Mahmoud, A. Hammoudeh, S. Gharaibeh, J. Melsheimer, *J. Mol. Catal. A: Chem.* 178 (2002) 161–167.
- [26] X. Yang, L. Wu, L. Ma, X. Li, T. Wang, S. Liao, *Catal. Commun.* 59 (2015) 184–188.
- [27] K. Wąsikowska, P. Dmowska, N. Bączek, K. Strzelec, J. Pernak, B. Markiewicz, *Pol. J. Chem. Technol.* 15 (2013) 28–32.
- [28] M. Lashdaf, A.O.I. Krause, M. Lindblad, M. Tiitta, T. Venäläinen, *Appl. Catal. A: Gen.* 241 (2003) 65–75.
- [29] J. Albadri, A. Alihoseinzadeh, A. Razeghi, *Catal. Commun.* 49 (2014) 1–5.
- [30] K.S. Prasad, H.B. Noh, S.S. Reddy, A.E. Reddy, Y.B. Shim, *Appl. Catal. A: Gen.* 476 (2014) 72–77.
- [31] X. Huang, X. Wang, M. Tan, X. Zou, W. Ding, X. Lu, *Appl. Catal. A: Gen.* 467 (2013) 407–413.
- [32] A. Frassoldati, C. Pinel, M. Besson, *Catal. Today* 203 (2013) 133–138.
- [33] A. Villa, M. Plebani, M. Schiavoni, C. Milone, E. Piperopoulos, S. Galvagno, L. Prati, *Catal. Today* 186 (2012) 76–82.
- [34] Z. Ma, H. Yang, Y. Qin, Y. Hao, G. Li, *J. Mol. Catal. A: Chem.* 331 (2010) 78–85.
- [35] H. Wang, S.X. Deng, Z.R. Shen, J.G. Wang, D.T. Ding, T.H. Chen, *Green Chem.* 11 (2009) 1499–1502.
- [36] Z.S. Hou, N. Theyssen, A. Brinkmann, K.V. Klementiev, W. Grunert, M. Buhl, W. Schmidt, B. Spliethoff, B. Tesche, C. Weidenthaler, W. Leitner, *J. Catal.* 258 (2008) 315–323.
- [37] F. Benetollo, R. Bertani, C. Bombieri, L. Toniolo, *Inorg. Chim. Acta* 233 (1995) 5–9.
- [38] A. Fabrello, A. Vavasori, F. Dall'Acqua, L. Toniolo, *J. Mol. Catal. A: Chem.* 276 (2007) 211–218.
- [39] A.I. Vogel, *A Text-Book of Practical Organic Chemistry*, third ed., 1956.
- [40] E.O. Stejskal, J. Schaefer, M.D. Sefcik, R.A. McKay, *Macromolecules* 14 (1981) 275–279.
- [41] J.G. Powles, J.H. Strange, *Proc. Phys. Soc.* 82 (1963) 6–15.
- [42] G.E. Pake, *J. Chem. Phys.* 16 (1948) 327–335.
- [43] D.C. Look, I.J. Lowe, J.A. Northby, *J. Chem. Phys.* 44 (1966) 3441–3452.
- [44] P.M.A. Sherwood, in: D. Briggs, M.P. Seah (Eds.), *Practical Surface Analysis*, Wiley, New York, 1990, p. 181.
- [45] P.A. Ramachandran, R.V. Chaudhari, *Three Phase Catalytic Reactors*, Gordon and Breach Science Publisher, New York, 1983.
- [46] C.V. Rode, R.V. Chaudhari, *Ind. Eng. Chem. Res.* 33 (1994) 1645–1653.
- [47] R.H. Perry, D.W. Green, *Perry's Chemical Engineers' Handbook*, sixth ed., McGraw-Hill International Editions, Chemical Engineering Series, New York/Singapore, 1984.
- [48] P.M. Cukor, J.M. Prausnitz, *J. Phys. Chem.* 76 (1972) 598–601.
- [49] A.A. Silva, R.A. Reis, M.L. Paredes, *J. Chem. Eng. Data* 54 (2009) 2067–2072.
- [50] C.D. Thompson, R.M. Rioux, N. Chen, F.H. Ribeiro, *J. Phys. Chem. B* 104 (2000) 3067–3077.
- [51] V.Z. Radkevich, T.L. Senko, K. Wilson, L.M. Grishenko, A.N. Zaderko, V.Y. Diyuk, *Appl. Catal. A: Gen.* 335 (2008) 241–251.
- [52] P. Gallezot, D. Richard, *Catal. Rev. Sci. Eng.* 40 (1/2) (1998) 81–126.
- [53] Z.C. Zhang, X. Zhang, Q.Y. Yu, Z.Z.C. Liu, C.M. Xu, J.S. Gao, J. Zhuang, X. Wang, *Chem. Eur. J.* 18 (2012) 2639–2645.
- [54] K. Chizari, I. Janowska, M. Houlle, I. Florea, O. Ersen, T. Romero, P. Bernhardt, M.J. Ledoux, C. Pham-Huu, *Appl. Catal. A: Gen.* 380 (2010) 72–80.
- [55] J. Chen, Q.H. Zhang, Y. Wang, H.L. Wan, *Adv. Synth. Catal.* 350 (2008) 453–464.
- [56] A. Villa, D. Wang, N. Dimitratos, D. Su, V. Trevisan, L. Prati, *Catal. Today* 150 (2010) 8–15.
- [57] N. Dimitratos, A. Villa, D. Wang, F. Porta, D. Su, L. Prati, *J. Catal.* 244 (2006) 113–121.